Detection of Faulty High Speed Wind Turbine Bearing Using Signal Intensity Estimator Technique

Mohamed Elforjani [a], Suliman Shanbr [b] and Eric Bechhoefer [c]
[a] University of Hertfordshire, AL10 9AB, UK, elforjani@gmail.com or m.elforjani@hert.ac.uk
[b] Cranfield University, Bedfordshire, UK
[c] Green Power Monitoring Systems, LLC, Vermont, USA

Abstract— Bearings are typically used in wind turbines to support shafts and gears that increase rotational speed from a low speed rotor to a higher speed electrical generator. For various bearing applications, condition monitoring using vibration measurements has remained a subject of intense study to the present day since several decades. Various signal processing techniques are used to analyze vibration signals and extract features related to defects. Statistical indicators such as Crest Factor (CF) and Kurtosis (KU) were reported as very sensitive indicators when the presence of the defects is pronounced, whilst their values may come down to the level of undamaged components when the damage is well advanced. Further, these indicators were applied to an acquired data from proposed diagnostic models, test rigs and instrumentations that were specifically employed for particular research tests, and thus it is essential to undertake further investigations and analysis to assess the influence of other factors such as the structural noise and other operating conditions on the real world applications. With this in mind, the present work proposes Signal Intensity Estimator (SIE) as a new technique to discriminate individual types of early natural damage in real world wind turbine bearings. Comparative results between SIE and conventional indicators such as KU and CF is also presented. It was concluded that SIE has an advantage over the other fault indicators if sufficient data is provided.

Index Terms— Wind Turbine, Condition Monitoring, Bearings, Vibration Measurements, Statistical Indicators, Signal Intensity Estimator, Kurtosis, Crest Factor.

I. INTRODUCTION

Wind power generation is more economical than nuclear and thermal power generation, and it is rapidly growing as a source of clean energy. Natural wind is available free of charge, so the main costs for wind power generation are construction and maintenance. To keep wind turbines function at optimal levels to efficiently harness and convert wind energy to electricity, condition monitoring of wind turbine components (e.g. bearings) is important because any wear, if is not caught in time, may lead to breakage of other adjacent parts. Vibration is the most regularly measured condition parameter in rotating machinery, and it is continuously monitored in many important applications. The commonly monitored vibration signals are displacement, velocity, and acceleration and the most basic vibration monitoring technique is to measure the overall vibration level over a broad band of frequencies. Researches on the use of vibration measurements for various applications shafts, bearings, gearboxes, compressors, motors, turbines (gas and steam) and pumps, are dated to before the turn of the 21st century. Vibration waveforms can be analyzed using the time and frequency domains. There are several time and frequency domain techniques used to analyze vibration signals. The main methods include calculation of enveloping curves, time series analysis, Fast Fourier transform (FFT), Gabor transform, Wigner Ville distribution, and wavelet transform [1]. Signals can also be characterized by statistical averaged parameters such as RMS, Mean, Variance, Skewness, Kolmogorov-Smirnov Test (k-s test), Energy Index (EI) or Kurtosis.

In addition to well-established patents, an enormous amount of work has been performed on developing machine diagnostics and studying failure processes. Many researchers have reported successful results for detecting damaged machine components through spectral analysis. Taylor [2] could establish a method for measuring the size of the defects on the raceways and formulate the sequence of appearing and disappearing spikes in the spectrum. Another diagnosis technique for differentiating the amplitude of healthy spectra from the damaged spectra was introduced by Mathew et al [3]. Further, investigation of fatigue cracks in gears employing amplitude and phase demodulation was undertaken by McFadden [4]. It was reported that gear health condition is directly proportional to the performance of the machinery. In another study, Randall [5] could classify the vibrations generated by gear meshing. In this study, it was shown that deviations from the ideal tooth profile produce a vibration signal at the tooth-meshing frequency. Also, variations in tooth loading will generate amplitude modulation whilst fluctuations in the rotational speed and/or non-uniform tooth spacing produce frequency modulation effects. Additional impulses can also be observed due to the local tooth faults.

A novel method for detection the gear damage was developed by Polyshchuk et al. [6]. In this method, a new gear fault detection parameter that is highly dependent on the energy change in the time frequency analysis was used. Lin et al. [7] employed an adaptive wavelet filter based on Morlet Wavelet. Parameters in the Morlet wavelet function are optimized based on the kurtosis maximization principle. It was postulated that the used adaptive wavelet filter was very effective in detection of signs originating from vibrations of a gearbox with fatigue tooth crack. Another analysis technique, independent component analysis (ICA), in frequency domain and wavelet filtering for gearbox fault diagnosis was used by Tian et al. [8]. Yu et al. [9] reported that the use of Hilbert-Huang transform can offer an accurate energy frequency time distribution that can be used to identify the gear conditions. Unique discussion about the condition monitoring of worm

gears to ensure reduction in costly unscheduled machine down time and explore the possibility of monitoring seeded defects on worm gears with vibration analysis was presented by Elforjani el al. [10]. Guoji et al. [11] applied bi-spectrum method to analyze vibration signals from helicopter gearbox. Modulation phenomena related to the local defect in the employed gear was behind the observed peaks in the bi-spectrum along the harmonic meshing frequencies.

Yang et al. [12] also utilized the artificial bee colony algorithm for optimizing support vector machines (SVM) parameters that were used for detection of gearbox faults. Further, comparative results between artificial bee colony algorithm and genetic algorithm showed that artificial bee colony algorithm could provide higher accuracy. Ensemble empirical mode decomposition for signal processing and feature extraction was employed by Rajeswari et al. [13]. For classifications of gear conditions, hybrid binary bat algorithm and machine learning algorithms were utilized. Jinxiu el al. [14] proposed a novel intelligent method based on dual-tree complex wavelet packet transform (DTCWPT) and multiple classifier fusion. This technique was employed in mechanical fault diagnosis for identifying fault categories. Authors claimed that the proposed technique could achieved high accurate results. Večeř et al. [15] applied frequently used condition indicators such as RMS, peak, energy operator, energy ratio, kurtosis etc. to vibration signals originating from manual transmission with helical gears during durability test. It was concluded that fault indicators such as RMS, crest factor and peak can provide a good track of the overall vibration level. In further study, Večeř et al. [16] utilised Kohonen Neural Networks and Adaptive-Network-based Fuzzy Interface System (ANFIS) as advanced classifiers for gearbox health conditions.

Comprehensive review for various condition indicators used for gear fault diagnosis was made by Sharma et al. [17]. Although the complexity in its mathematical notations, Spectral Kurtosis (SK) is considered as one of the well-established techniques that are widely used for monitoring machine health conditions. To detect and characterize the signal transients, Dwyer [18] originally defined the SK on the real part of bank output from Short Time Fourier Transform (STFT) filter. To employ the SK for non-stationary processes, Antoni [19] formulated the SK using Wold-Cramér decomposition. Bechhoefer et al. [20] developed three statistical models to define a gear health indicators (HI) as a function of condition indicators (CI); order statistics (max of n CIs), sum of CIs and normalized energy. It was concluded that gear health indicators showed good performance in detection of pitting damage on gears.

For the condition monitoring of wind turbine applications, there is a growing attention being given to the maintenance of the installed wind turbines. Available commercial condition monitoring techniques used for wind turbines and practical challenges were discussed by Yang et al. [21]. It was concluded that further research work on non-linear signals and analysis of time-domain or frequency-domain signal changes under incipient fault conditions should be undertaken. Bangalore et al. [22] proposed a method using Mahalanobis distance (MHD) to overcome the errors from the Artificial Neural Networks (ANN) models due to discontinuity in supervisory control and data acquisition (SCADA). The MHD correlates the error from the ANN model and the operating conditions. The proposed method was applied to four wind turbine case studies with faulty gearboxes. Bangalore et al. postulated that the proposed method could improve the anomaly detection in the ANN model. In another work Bryant et al [23] developed an asset model for offshore wind turbine reliability. To capture the stochastic nature of the dynamic processes with the considering of degradation, inspection and maintenance processes, this model was developed based on the Petri net method. A Monte Carlo simulation procedure was applied to the model, and relevant statistics were collected enabling various maintenance scenarios. Authors of this work reported that the developed model could efficiently manage wind turbine assets.

Evaluation study of several available condition monitoring algorithms such as frequency domain, cepstrum analysis, time synchronous averaging narrowband and residual methods, bearing envelope analysis and spectral kurtosis for wind turbine applications was undertaken [24]. A full-scale baseline wind turbine drive train and a drive train with several gear and bearing failures were tested at the National Renewable Energy Laboratory (NREL). The study highlighted the feasibility of each algorithm to accurately detect the bearing and gear wheel component health. Monitoring of wind turbine gearboxes was investigated by Feng et al. [25]. The study presented a summary of different failure modes in wind turbine gearboxes. Review of commercial approaches such as supervisory control and data acquisition (SCADA) and condition monitoring system (CMS) was presented. Authors recommended that SCADA should be integrated with CMS to efficiently detect wind turbine gearboxes failure. A vibration approach based for condition monitoring of wind turbine drivetrain components was proposed by Luo et al. [26]. To correlate the damage features with vibration signals originating from bearings and gears, both spectral analysis and acceleration enveloping techniques were employed. For constant operating conditions, specific damage features were detected using synchronous analysis.

II. Motivation and Novelty

Modern rotating machines are fatigue loaded machines (e.g. wind turbines) and operational experience with these machines manifested that their components are failing at abrupt high rates. For instance, bearings experience several types of repairable damage including micro-pitting or “gray staining,” abrasive wear, foreign object debris damage, surface corrosion, and fretting corrosion. This has led the engineers and scientists to develop online condition monitoring schemes and fault detection technologies for early forewarning of incipient mechanical and electrical faults. Most published work showed that vibration monitoring is currently favoured in the proposed available systems using standard time and frequency domain techniques for analysis.

However, accurate and reliable fault detection schemes for rotating machines remain a challenge due to the complexity in mechanical systems, complexity of the developed tools and feasibility of these tools to detect and characterize non-stationary signals in the case of varying operation conditions

(e.g. wind turbines). Further, most of the techniques documented and reported up-to-date in the literature have only been applied to specifically designed small-scale test-beds and unique specimens and therefore their effectiveness, both technically and economically, has to be proved with further investigations in the real world applications. The challenge in the applicability of these techniques is the need of proper understanding of their very complex and sophisticated algorithms and mathematical notations and therefore to apply such techniques well educated and experienced users are required. Also, selection of suitable window sizes to avoid the losses in time localization and/or frequency localisation in the analysis of condition monitoring data represents another issue when these techniques are used. Failure in selection the right window size may lead to false alarms and fake results. To overcome this issue a proper window size must appropriately be selected. This is not an easy task as off the shelf, there is no a global acceptance for selecting reasonable window sizes for different applications. As a result of this, process of trial and error using different window sizes are primarily dependent on both the type of application and the experience of the analysts who should make efforts to eventually get satisfactory results. This is in turn subject to human errors and a time consuming. Thus, there is still an on- going need for providing more efficient ways for the diagnosis and prognosis of vibration signals and more ways for measuring deviations from the normal conditions.

To respond to these, this work presents a new technique, Signal Intensity Estimator (SIE) to monitor real world applications such as wind turbines in less time consuming, more efficient and simple use. The feasibility of SIE in monitoring the real world applications dose not only include the correlation of the natural wear developed on the machine components with the corresponding measured vibration signals in both time domain and frequency domain representations, as it charts the general trend at any period of time using the cumulative sum method, but also it offers the solution for selecting the window sizes. With the known of the application type (e.g. bearings, gears, etc), the sampling frequency and the rotational speed, the SIE technique will choose the most appropriate window size and accordingly detect and locate any machine component fault.

III. Data Measurements and Features Extraction

Real world wind turbine (S88, Suzelon) with an output power of 2 MW was equipped to measure vibration signals originating from faulty bearing inner race. The high speed shaft is driven by a 20 tooth pinion gear and is supported by the high speed stage bearings located on the front and back sides of the shaft, which makes 1800 revolutions per minute during power generation. The acquisition system was continuously set to acquire the vibration waveforms from the faulty bearing with increasing in severity for 50 consecutive days. After 50 days of measurements the bearing was bore-scoped and visual inspection showed a fault has occurred on the bearing inner race, see figure 1. Two data sets involve radial vibration measurements acquired from the high speed bearing and tachometer data were provided by [27]. Vibration signals was acquired from one radial accelerometer channel in (g) with a sampling rate of 97.656 kHz and recording time of 6 seconds. One tachometer channel was employed to measure the rotational speed with a sampling rate of 2/rev (constant angular sampling) and approximately recording length of 40 seconds. Another measurements involve the vibration energy for 66 days (starts from February 25, 2013 to May 01, 2013) were also provided.

The wind speed acting on the wind turbine varies depending on the influences of land features, the height from the ground and turbulence caused by changes in the weather. The bearing loads and rotating speeds vary considerably due to constantly changing winds. At wind speeds below the cut-in wind speed (i.e. the minimum wind speed required for power generation), the rotor shaft will idle resulting in low-speed, low-load operation. At wind speeds above the cut-in speed, the rotating speed increases above the rated speed, resulting in average loads. In the case of wind gusts, the blades and rotor will exert large loads on the rotor shaft bearing. Such changes in the load, moment and rotating speed also affect the gearbox bearings. One of the features of wind turbine bearings is that they operate in a wide range of loads from light to heavy load. Figure 2 shows the variation in the measured average speed over 50 days of measurements. It can be observed that the readings from the tachometer channel show an instantaneous shaft speed ranging from 29.2 Hz in day 7 to a maximum of 31.3 Hz in day 12 whilst the overall average speed throughout 50 days of measurements was 30.36 Hz, see figure 2.

Figure 1 Surface Damage on Bearing Inner Race, See 'Circle' Section

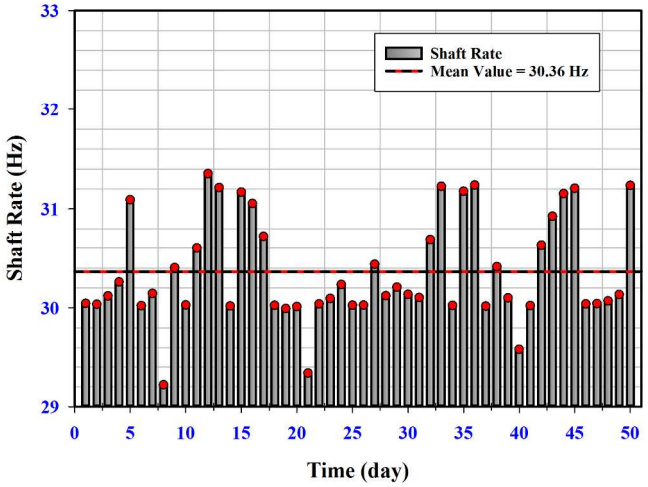

Figure 2 Variation in Shaft Rate

Thus, the acquired signals, required for the condition monitoring analysis, are expected to be non-stationary signals. These signals are very often complex to analyze as their features rapidly vary over microseconds. To identify the type of the acquired signals, statistical quantities of vibration waveforms were calculated. In addition to the features such as mean, standard deviation, median and percentile, normality tests were also performed. Three tests Kolmogorov-Smirnov, Lilliefors, and Jarque-Bera to determine normality of the data were used. Clear evidence of non-stationery signals was observed from the results, presented in figure 3, as these results show that the variance of the acquired waveforms changes with time and all results obtained from the normality tests suggested not normal waveforms were recorded.

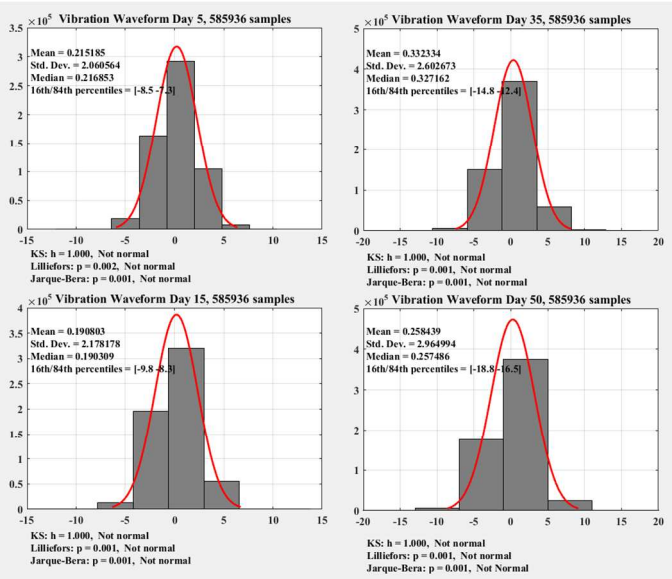

Figure 3 Results of Statistical Analysis and Normality Tests

As a consequence of this, the change in the output speed may probably lead to a significant variation in the location of the forcing frequencies, corresponding to the bearing components, in the vibration spectrum; making the identification of the faulty component too difficult. However, this issue can be resolved if a reliable and robust analysis technique, which can eventually adopt the variation in the operating conditions, is provided, see the following sections. Typical vibration waveforms that reflect the general trend throughout the 50 days of measurements are presented in figure 4. Though the recorded waveforms show high vibration levels throughout the last days of measurements, transient events in these waveforms, recorded from the faulty bearing, can hardly be seen. This can be attributed to the fact that the transient events were superimposed by the noise and signal interference, originating from the adjacent components.

Observations of continuous monitoring of the energy rate levels for 66 days (1584-hours) of bearing operation are presented in figures 5. It was observed that at approximately 400-hours into operation energy levels from the shaft-tick and the bearing inner race began to increase steadily. This was not observed in the other bearing components though energy levels from the bearing cage significantly increased after 1500-hours of operation; much later that was observed in the shaft-tick and the bearing inner race. This in turn suggested that there is a damage occurred on the bearing inner race and probably another damage on the bearing cage; relevance of this will be evident later in the paper. The increase in energy levels in the bearing cage and the bearing inner race from earlier in the operation period between 300 to 600-hours to the condition of surface damage was in the order of 40% and 550% respectively, see figure 5.

Bearings with rolling elements generate several frequencies which can be calculated and detected if the physical dimensions of the bearings and the RPM (Revolution per Minute) at which they are running are known.

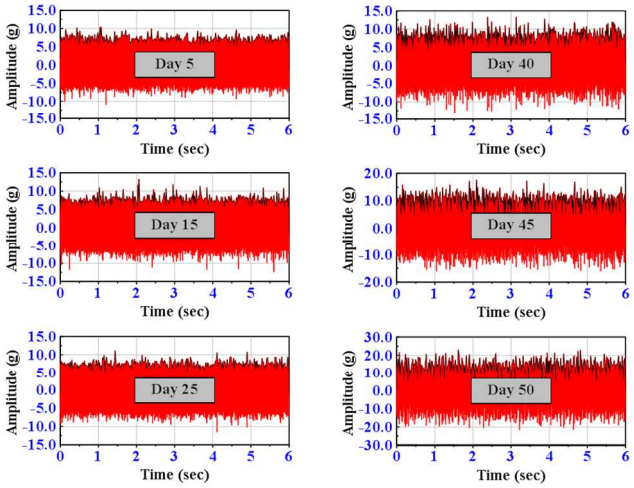

Figure 4 Typical Vibration Waveforms

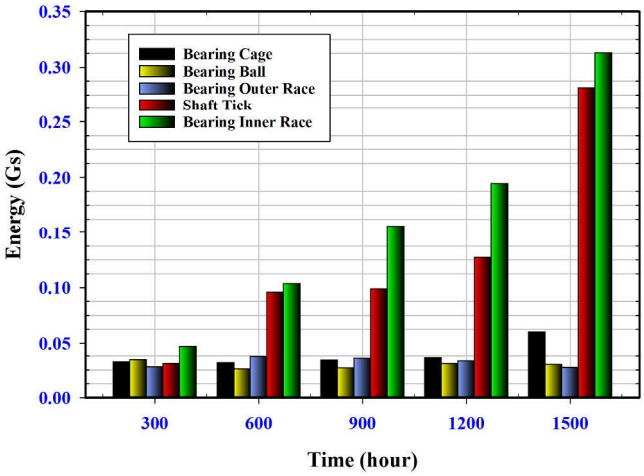

Figure 5 Energy rate levels for 66 days

These frequencies can be recorded with an accelerometer and a spectrum analyzer. There are four stages in bearing failure that can be detected with vibration analysis [28 and 29]. These stages include normal operation stage which can be observed at ultrasonic frequencies whilst the frequencies of the second stage are noted in the middle of the spectrum. It is

worth mentioning that throughout the second stage defects begin to ring bearing components natural frequencies. In the third stage of failure, bearing defect frequencies and harmonics clearly appear on the spectrum. These frequencies are corresponding to the defects in the rolling elements. The last stage of the failure appears when the bearing approaches its end of life. In this stage, random high frequency vibration spikes, all running together, are noted on the spectrum. Frequency related to vibration can be described as the number of times an impact occurs during a specific period and it is measured in Hertz (cycles per second) and CPM (cycles per minute, 1 Hz = 60 CPM).

Predominant frequencies generated by bearings consist of Bearing Outer Race Frequency (BPFO), Bearing Inner Race Frequency (BPFI), Ball Spin Frequency (BSF) and Fundamental Train Frequency (FTF). When bearings begin to fail, these frequencies and multiples of these frequencies show up as spikes on a vibration analysis spectrum. All data are based on 1 RPM and with the known of number of rollers (n), rotor speed (f_r), contact angle (Θ), pitch diameter (d_p) and the ball diameter (d_b), the following equations are used to estimate BPFO, BPFI, BSF and FTF in Hertz [29].

$$BPFO = \frac{n}{2} f_r \left(1 - \frac{d_b}{d_p} \cos\theta \right) \quad (1)$$

$$BPFI = \frac{n}{2} f_r \left(1 + \frac{d_b}{d_p} \cos\theta \right) \quad (2)$$

$$BSF = \frac{d_p}{2d_b} f_r \left(1 - \frac{d_b^2}{d_p^2} \cos\theta \right) \quad (3)$$

$$FTF = \frac{f_r}{2} \left(1 - \frac{d_b}{d_p} \cos\theta \right) \quad (4)$$

The cage, ball elements, inner race and outer race rates are 0.42, 2.87, 9.46, 6.72 respectively [27]. Consider the effect of the variation in the shaft speed on the spectral content of a bearing fault frequency, the range of fault frequencies during days 10, 20, 30, 40 and 50 is presented in table 1. It should be noted that these frequency components was estimated using the average speed recorded by the tachometer.

TABLE 1 CHARACTERISTIC FREQUENCIES OF BEARING COMPONENTS (Hz).

Bearing Component	Day				
	10	20	30	40	50
Cage	12.61	12.60	12.66	12.43	13.12
Ball	86.18	86.13	86.48	84.90	89.64
Inner Race	284.00	283.90	285.00	279.86	295.48
Outer Race	201.79	201.67	202.50	198.80	209.89

There are standard statistical features that can characterize the trend of the data. These features include mean, standard deviation, kurtosis, crest factor and RMS. For continuous monitoring, Elforjani [30] showed that employing techniques such as kurtosis and crest factor would not offer the operator a sensitive tool for observing high transient type activity. Further, in the condition monitoring applications, the commonly used RMS concerns only a period of time and therefore some short transient events may be lost. RMS is typically recorded over a predefined time constant. As such the RMS values are not necessarily sensitive to transient changes, which typically are of a few micro-seconds. To overcome this inadequacy, Signal Intensity Estimator (SIE) that is relatively more sensitive was developed by Elforjani [30]. This statistical indicator is highly based on the cumulative sum (CUSUM) of a given sample that is now one of the most well-known monitoring methods for sequential data [31]. CUSUM not only allows the total to be stated at any point in time without having to sum the entire sequence but also it can save having to record the sequence itself, if the particular activities are not individually important. Processing several samples from failure histories using cumulative sums will result in greater sensitivity for detecting shifts or variation in trends over time.

SIE, is used to measure the intensity levels of segments in a given time domain signal over a time period. Formally, SIE can be defined as the ratio of the sum of cumulative sum of a defined segment, window, ($SCS_{segment}$) in a given time domain signal to the overall root mean square ($RMS_{overall}$) of the same signal. This normalization will allow the user to perform any analysis for any condition monitoring data (e.g. vibration, Acoustic Emission, etc.) irrespective of their physical units and also enhances the resulting SIE values without the need for an enhancement factor. In application, SIE value of one, between two adjacent segments, is associated with non-transient type signals and greater than one, either in the form of high amplitude levels and/or higher-frequency components, where transient characteristics are present. For other segments with relatively lower level of activities, SIE will be less than one. High intensity concentration in a given segment can be considered as an early forewarning of incipient mechanical and/or electrical faults.

The advantage of the SIE over the classical envelope is that the SIE is a normalized piecewise segment technique whilst the envelope is based on the entire signal. This means that the SIE not only displays the ratio of the total at any given time but also it can chart statistic that involves current and previous data values from the process. This helps to track how the sample values deviate from a target value and also improves the ability to detect micro-changes. In its previous version, Elforjani [30 and 32] has successfully applied SIE for continuous condition monitoring of degrading bearing using Acoustic Emission technique. In the same work, Elforjani has also employed the SIE as a solely extracted feature from the recorded AE signals throughout bearing tests to develop machine learning models, which were successfully used to estimate the remaining useful time of bearings. To efficiently perform further time and frequency domain signal processing, improvements and updates were made to the calculation method of the SIE. This involved the ability to select the type

of application, ability to calculate the proper maximum frequency of analysis, efficient calculation of segment size and perform the FFT and calculation of the spectral power of signals. Figure 6 summarizes in sufficient details the calculation method of SIE from the basic steps until the final results. In most well-established condition monitoring analysis techniques, reasonable Maximum Frequency of analysis (F_{max}) and Lines of Resolution (LOR) should be set in the analyzer prior to any frequency analysis and therefore several attempts are made to achieve the optimal results. The proposed SIE method provides simple method of calculating F_{max} that can significantly help the analyst/user to avoid this indefinite settings.

To calculate the SIE, signals are first rectified and with the known of application type, sampling rate frequency (F_S) and the rotational speed (RPM) the maximum frequency of analysis (F_{max}) can be calculated using the following equation.

$$F_{max} = \beta.\frac{RPM}{60} \quad (5)$$

For good frequency localization results and monitoring the frequencies of interest, F_{max} should always be less than the Nyquist Frequency (NF). The constant β, in the previous equation, is highly dependent on the type of application. The calculated F_{max} values are then compared with the suggested values in table 2. The suggested values of F_{max} were determined from long iterative analysis using different values of β = {20, 40, 60, 80 and 100}. The optimal values of β for bearing and gear applications was found to be 40 and 80 respectively. These values were successfully applied to different types of rotating machines.

TABLE 2 SELECTED VALUES OF MAXIMUM FREQUENCY OF ANALYSIS.

Application Type	β	F_{max} (Hz)	
		Calculated [a]	Selected [b]
Bearings	40	$F_{max} < 800$	Equal to F_{max} [c]
Bearings	40	$800 \leq F_{max} \leq 1500$	1000 - 2000
Bearings	40	$F_{max} > 1500$	2000 - 4000
Bearings	40	$F_{max} > F_S$	< NF [d]
Gears	80	$F_{max} < 800$	Equal to F_{max}
Gears	80	$800 \leq F_{max} \leq 1500$	2000 - 4000
Gears	80	$F_{max} > 1500$	4000 - 6000
Gears	80	$F_{max} > F_S$	< NF

a. This value is calculated using equation (5).
b. This value is selected based on the calculated value to obtain the optimal frequency localisation.
c. The calculated value is selected if it is less than 800 Hz.
d. The selected value is set to be less than the Nyquist Frequency if the calculated value is greater than the sampling rate frequency.

When the proper value of F_{max} is decided, the next step involves the calculation of number of segments and accordingly the size of each segment. Equation 6 is employed to calculate the size of each segment.

$$n_{segment} = \frac{F_S}{F_{max}} \quad (6)$$

To determine the values of SIE from a given signal, two approaches can be employed. The first method (equation 7) involves the direct extraction of the SIE values from the time domain data, while in the second method (equation 8) the SIE is determined using the extracted frequency components from the signal. The resulting SIE values using the second method are more enhanced.

$$SIE_T = \frac{SCS_{segment}}{RMS_{overall}} \quad (7)$$

$$SIE_F = \sum \left| FFT\left(\frac{CS_{segment}}{RMS_{overall}} \right) \right| \quad (8)$$

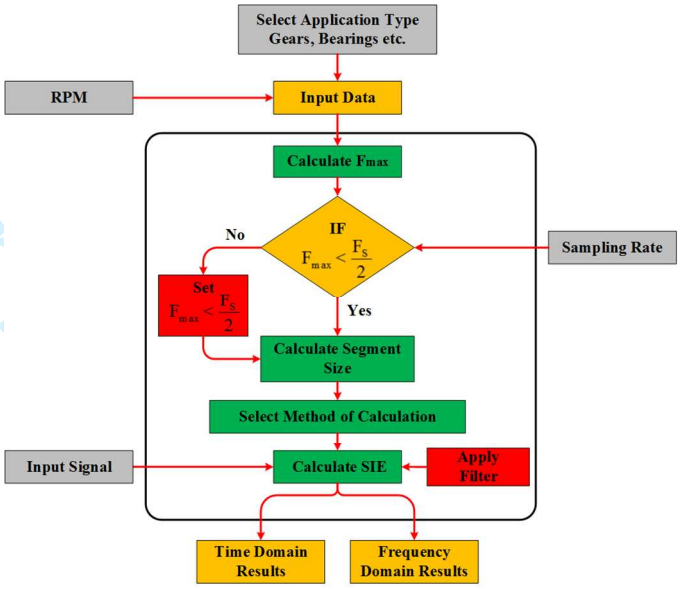

Figure 6 Steps for Calculating SIE

To show the advantages of SIE over the widely used fault indicators, both the Kurtosis (KU) and the Crest Factor (CF) were also calculated in the same manner. For every individual segment and with the known of individual event (x), segment size (n), segment mean (μ) and segment standard deviation (σ), KU and CF were calculated using equations 9 and 10 respectively [33]. To further de-noise the resulting SIE, KU and CF values a filter (low pass filter, band pass filter or high pass filter) can be used.

$$KU = \frac{1}{n}\sum_{i=1}^{n}\left(\frac{x_i - \mu_{segment}}{\sigma_{segment}} \right)^4 \quad (9)$$

$$CF = \frac{Peak_{segment}}{RMS_{segment}} \quad (10)$$

Thus far the steps have shown the method of calculating the SIE, KU and CF. To provide more ways for analyzing the signals and more ways for measuring deviations from the normal conditions, various time and frequency domain signal processing techniques are widely applied to the measured vibration waveforms. One of the most used signal processing techniques is the spectrum analysis where several frequency components and sidebands in the analysis of vibration signals can be identified. The use of the spectral analysis is particularly appropriate as it gives information about the measured vibration signals in frequency domain. For this particular work, frequency domain analysis using Power Spectral Density (PSD) was applied to the vibration waveforms. It is worth mentioning that for individual complex Fast Fourier Transform value (H) and sample size (N) the Power Spectral Density is calculated as Sum Squared Amplitude using the following equation:

$$Power = \frac{1}{N}\sum_{i=0}^{N-1}\left|H_i\right|^2 \quad (11)$$

IV. Analysis, Results and Discussion

Prior to the spectral analysis, vibration energy, acquired from continuous monitoring of the bearing inner race throughout 1584 hours operation, was employed to extract SIE, KU and CF values. To map the general transient trend, SIE, KU and CF were first calculated for every individual segment based on the selected F_{max} (2000 Hz) and then optimally fitted using the popular least-square method, shown in figure 7.

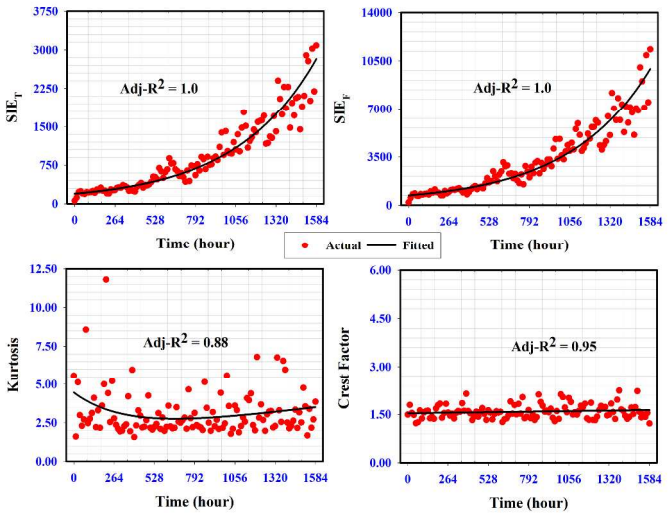

Figure 7 SIE, Kurtosis and Crest Factor

While the measurements passed 200-hours in operation, results indicated that the SIE has relatively high values. It is worth noting that after 500-hours to 800-hours all calculated SIE values steadily increased whilst KU and CF values remained almost constant. As the measurements progressed with time (1000-hours to 1500-hours) the SIE values were very sensitive to the variation in bearing signals, see figure 7; at 1584-hours in operation, maximum values of SIE were recorded. Also was noted that as the defect was well advanced after running 700-hours to 1584-hours, KU and CF showed steady trend though insignificant increase in CF was observed. This reinforces the widely acknowledged view that KU and CF are reliable indicators only in the presence of incipient defects while they did not respond enough to the significantly increasing damages in the bearing [30 and 33].

The fitted data was further processed to estimate the Remaining Useful Life (RUL) for the degrading bearing. Two supervised machine learning techniques; Regression Trees (RT) and Multilayer Artificial Neural Network (ANN) model were used to correlate vibration features with corresponding natural wear of the bearing throughout the measurements period. An ANN model containing one input layer with one input parameter, one output layer (RUL), and three hidden layers with (7-3-7) neurons, was iteratively selected. It is worth mentioning that the fitted data was randomly split into 75 % for training the prediction models and 25 % to test the proposed models. Prior to the training process, four models from regression techniques were constructed. Each model was fed with one solely vibration feature such as SIE, KU, and/or CF as an input parameter whilst the RUL was the output parameter. Equations 12 and 13 were used to estimate the RUL and the Error respectively [32].

$$RUL = t_f - t_i \quad (12)$$

$$Error = \frac{Actual(RUL) - Estimated(RUL)}{Actual(RUL)} \times 100 \quad (13)$$

The (t_f) is the time when the fully mature failure on the bearing race was formed; in this particular investigation this time was selected as the termination of the measurements period (1584-hours). The (t_i) is the instant time at which the remaining useful life was calculated.

Results of the estimation of the RUL are presented in figures 8 and 9. By visually inspecting the resulting plots, it can evidently be seen that the prediction models for SIE and CF could well estimate the RUL. Observations from the resulting plots of the test data show that the RUL values estimated by the RT and ANN models using SIE and CF as inputs are almost closer to the actual RUL line (a perfect concentration of estimated RUL values around the actual line is a clear evidence of low Error and thus an ideal model performance). Also was noted that both RT and ANN models for KU failed to predict RUL for the bearing throughout the measurements period between 800-hours to 1200-hours though relatively better results was obtained using RT model. Interestingly, the error results also show some negative error values calculated by the prediction models using the KU as input parameter. This is due to the overestimation of the RUL. Another clear evidence of the advantage of SIE and CF over the KU in estimating the RUL was the results obtained from the analysis of the standard error of the mean, presented in figure 10. With the known of the sample Standard Deviation

(σ) and the sample size (N), the Standard Error of the Mean (SEμ) was calculated using the following equation:

$$SE_{\mu} = \frac{\sigma}{\sqrt{N}} \quad (14)$$

In addition to the time domain analysis, the next phase of this investigation involved the application of PSD to the calculated SIE, KU and CF values. The measured vibration data comprises vibration waveforms recorded at days 5, 20, 35, and 50 were analyzed to investigate the periodicity of the transient nature of the vibration signals from the degrading bearing.

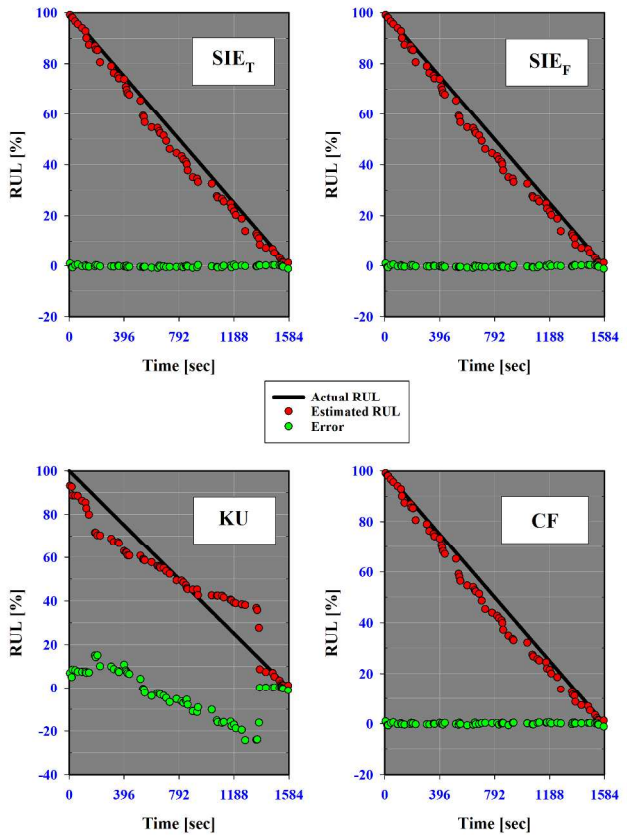

Figure 8 Results of RUL and Error (RT Model)

The power spectrum results of vibration signals are highlighted in figures 11 to 14. It is very clear that as early as into the measurements (5 to 20 days) the resulting spectrum from both KU and CF is significantly difficult to understand; there was a broad frequency spectrum of the vibration signals. However, this is not the case in the resulting spectrum of the SIE as clear early evidence of faulty inner race and cage was observed during day 5, shown in figure 11. Also was noted that SIE spectrum could show an evidence of cage fault components (1x-FTF ≈ 12.07 Hz, 2x-FTF ≈ 24.14 Hz and 3x-FTF ≈ 36.21 Hz) after 5 days into measurements, see figure 11.

These components could not be identified throughout the following days of operation due to the noisy results. From 20 days into the measurements, the SIE could show more clear detection of the defect frequency, which was not observed in the KU and CF results, particularly the KU though CF could show the first sign of 1x-BPFI after 20 days of operation; much later that was detected by the SIE technique, see figures 13 and 14; observations from spectrum analysis revealed that KU method was relatively noisy than the other techniques on the basis that it could not resolve most of the frequency peaks. Further, SIE method has shown an advantage over the other techniques on the basis that it could locate large frequency components of 1x-BPFI and clear 2x-BPFI, see figures 11 to 14. It is also particularly interesting to note that on the termination of measurements (50 days); all techniques could show a clear periodicity of vibration events at (1x-BPFI ≈ 291 Hz), presented in figure 14.

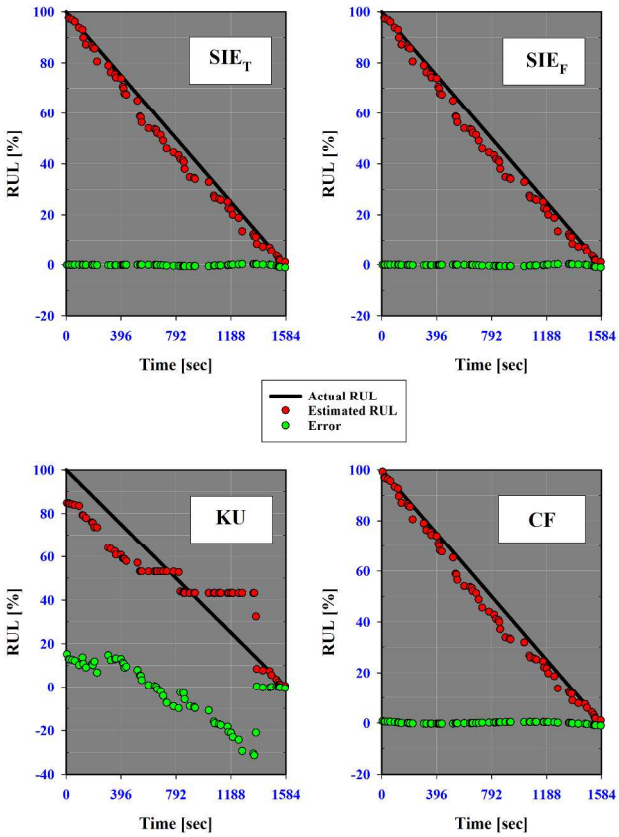

Figure 9 Results of RUL and Error (ANN Model)

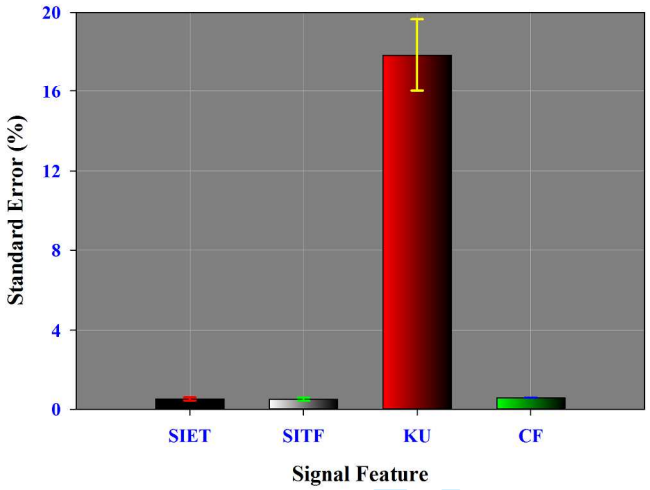

Figure 10 Results of Standard Error with Mean

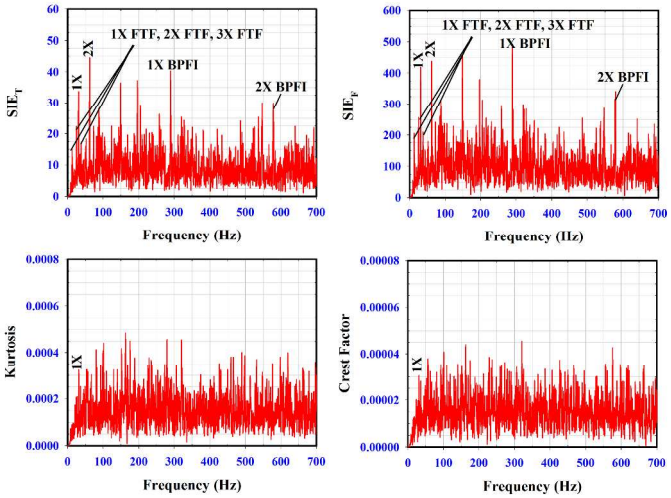

Figure 11 Results of PSD (day 5, 1x = 30.8 Hz)

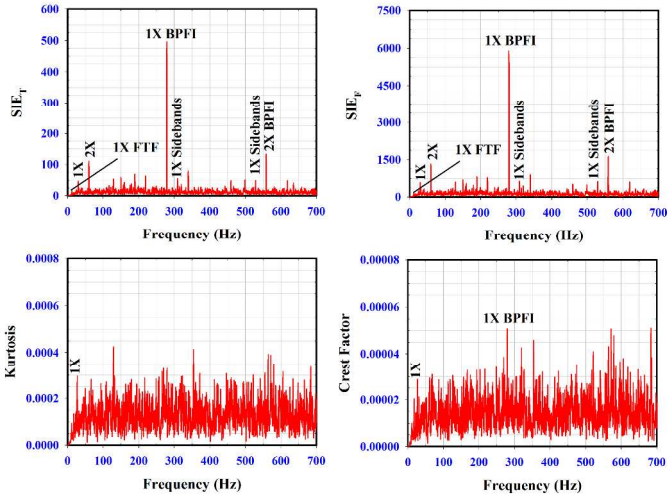

Figure 12 Results of PSD (day 20, 1x = 30 Hz)

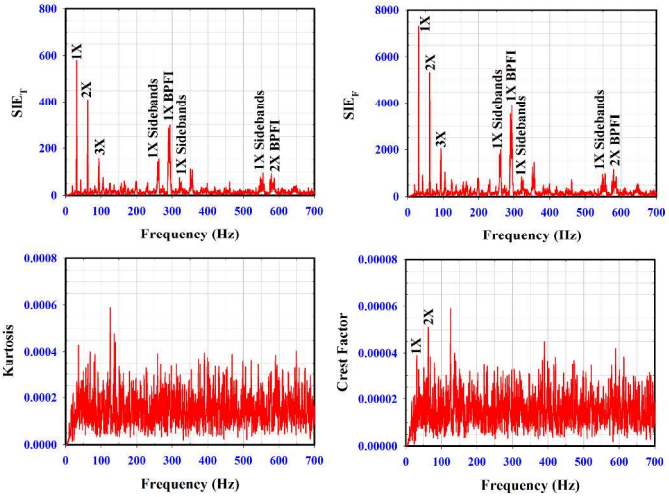

Figure 13 Results of PSD (day 35, 1x = 30.27 Hz)

To de-noise the results of SIE, KU and CF which were observed on the PSD, these indicators were also further analyzed using the nonlinear Eigen Frequency Estimation Algorithms (EFEA). The map of these algorithms can present a visual picture of the faulty bearing inner race as they offer true high-resolution frequency estimation. The procedures begin by generating an Eigen-decomposition from a data (trajectory) matrix using SVD (singular value decomposition). The data matrices can be forward prediction based (Fwd) or forward-backward prediction based (FB). The FB procedures are generally more accurate when estimating the frequencies of sinusoids. For damped sinusoids, the Fwd procedures will typically be more accurate. In this investigation the FB procedures were used and the results showed clear continuous increase in evidence of periodicity from waveforms (day 30, day 40 and day 50), presented in figures 15 to 17. Further, the results also confirms the author's belief that the SIE is reliable, robust and sensitive to the detection of incipient cracks and surface spalls and can successfully be employed for condition monitoring of rotating machines. Again these plots are another clear evidence of the advantage of SIE over the classical KU and CF.

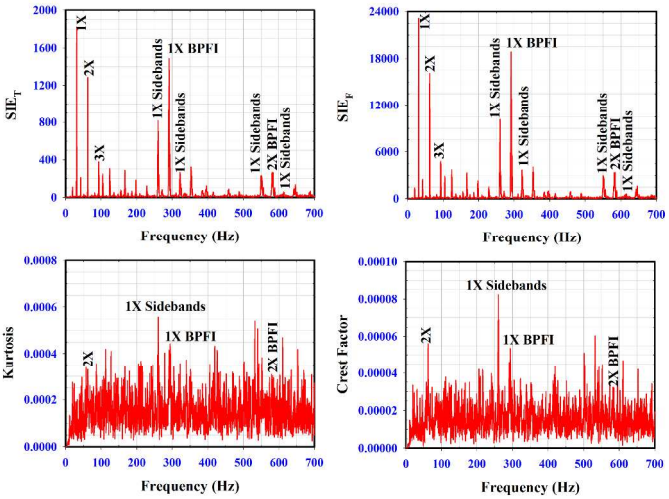

Figure 14 Results of PSD (day 50, 1x = 31.17 Hz)

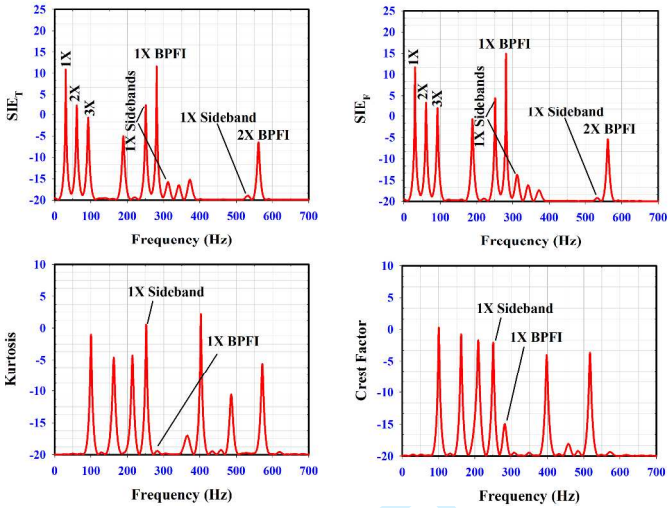

Figure 15 Results of EFEA (day 30, 1x = 30.17 Hz)

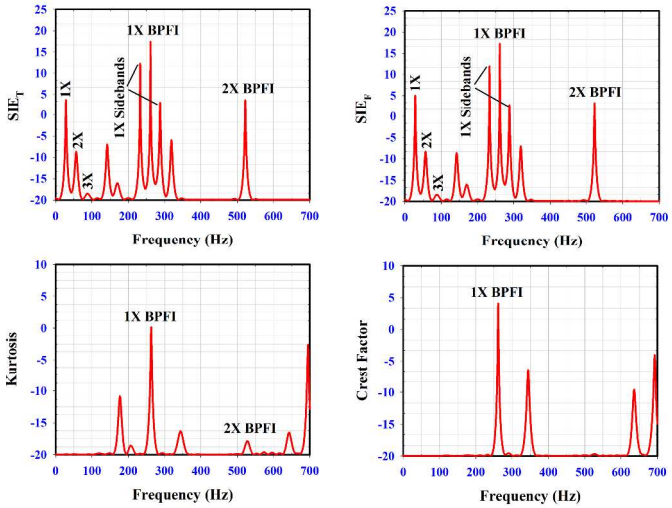

Figure 16 Results of EFEA (day 40, 1x = 28.17 Hz)

Lastly, as discussed in the previous sections the variation in the rotational speed has caused non-stationary signals which eventually led to different location of fault frequency components in the resulting vibration spectrum. The location of these components in the vibration spectrum could be identified for each day of measurements based on the rotational speed that was recorded during the period of acquiring the waveforms. To ascertain the obtained results by the SIE method, comparative results between the calculation of the fault frequency of the inner race using the tachometer readings and the calculation of the same fault frequency employing the SIE spectrum was also undertaken. This comparison involved the results obtained by the two methods for 10 days of measurements, presented in figure 18. Observations from this plot showed that there is a relative difference between the two approaches though a significant difference was noted in the measurements of day 40; (BPFI = 280.16 Hz at average 1x = 29.6 Hz) using the tachometer readings whilst (BPFI = 265.2 Hz at 1x = 28.17 Hz) obtained from the SIE spectrum. This difference is expected as the BPFI values by the tachometer were calculated using the average speed. This average speed does not necessarily represent the exact RPM for a specific period of given day at which vibration waveforms for that day was acquired. Further, for each day of measurements the waveforms were acquired over a time length of 6 seconds whilst tachometer readings were taken over a longer period of 40 seconds and therefore the exact value of RPM could be lower and/or higher than the average speed. This fact confirms that the obtained results by the SIE method are accurate.

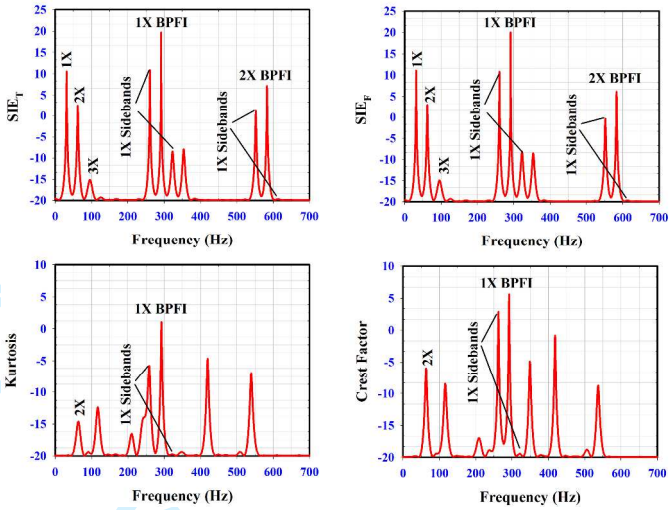

Figure 17 Results of EFEA (day 50, 1x = 31.17 Hz)

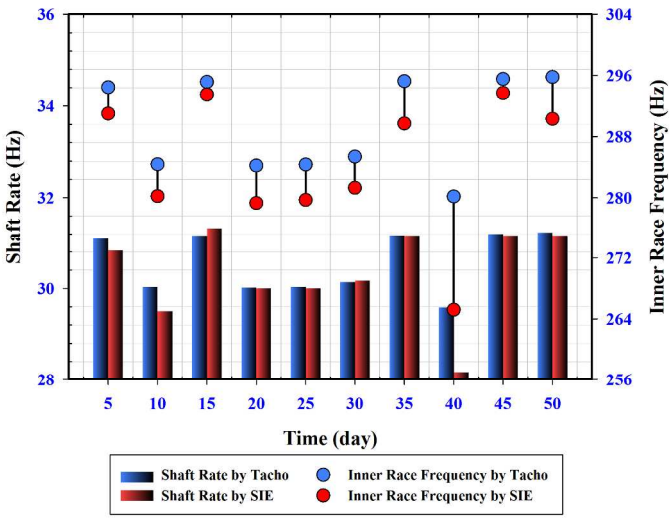

Figure 18 Results of BPFI using Tachometer Readings and SIE Method

V. Conclusion

It can be concluded that this study demonstrated the applicability of SIE technique in detecting and locating crack initiation and propagation on real world wind turbine bearings. This study successfully demonstrated the ability to accurately estimate the RUL for wind turbine bearings using the proposed RT and ANN models with SIE and/or CF as inputs parameters. It was also shown that by employing a range of data analysis techniques such as spectrum analysis (PSD and EFEA), the presence of a crack onset and its propagation can be detected by the SIE technique. Finally, the results from this investigation show that the method of identifying the faulty machine component can be employed as a quality control tool for bearing manufacturers particularly for testing bearing material homogeneity.

References

[1] Xiaoli, L.: A Brief Review: Acoustic Emission Method for Tool Wear Monitoring During Testing. International Journal of Machine Tools & Manufacturing, Volume 42, Issue 2 (2002)

[2] Taylor, J., I.: Identification of Bearing Defects by Spectral Analysis. Mechanical Design, Volume 102 (1980)

[3] Mathew, J., Alfredson, R. J.: The Condition Monitoring of Rolling Element Bearing Using Vibration Analysis. Vibration and Acoustics, Stress, and Reliability in Design, Volume 106 (1984)

[4] McFadden, P., D.: Detecting Fatigue Cracks in Gears by Amplitude and Phase Demodulation of the Meshing Vibration. Journal of Vibration and Acoustic, ASME, Volume 108 (1986)

[5] Randall, R., B.: A New Method of Modelling Gear Faults. Journal of Mechanical Design, ASME Volume 104 (1982)

[6] Polyshchuk, V., V, Choy, F., K., Braun, M., J.: Gear Fault Detection with Time Frequency Based Parameter NP4. International Journal of Rotating Machinery, Volume 8, Issue 1 (2002)

[7] Lin, J., Zuo, M., J.: Gear Box Fault Diagnosis Using Adaptive Wavelet Filter. Mechanical Systems and Signal Processing, Volume 17, Issue 6 (2003)

[8] Tian, X., Jing, L., Fyfe, K., R., Zuo, M., J.: Gearbox Fault Diagnosis Using Independent Component Analysis In The Frequency Domain And Wavelet Filtering. Proceedings of IEEE International Conference on Acoustics, Speech, and Signal Processing, Volume 2 (2003)

[9] Yu, D., Yang, Y., Cheng, J.: Applications of Time-Frequency Entropy Method Based on Hilbert Huang Transform to Gear Fault Diagnosis. Measurement, Volume 40, Issue 9 (2007)

[10] Elforjani, M., Mba, D., Muhammad, A., Sire, A.: Condition Monitoring of Worm Gears. Applied Acoustics, Volume 73, Issue 8 (2012)

[11] Guoji, S., McLaughlin, S., Yongcheng, X., White, P.: Theoretical and Experimental Analysis of Bispectrum of Vibration Signals for Fault Diagnosis of Gears. Mechanical Systems and Signal Processing, Volume 43, Issue 1 (2014)

[12] Yang, D., Liu, Y., Li, S., Li, X., Ma, L.: Gear Fault Diagnosis Based on Support Vector Machine Optimized by Artificial Bee Colony Algorithm. Mechanism and Machine Theory, Volume 90 (2015)

[13] Rajeswari, C., Sathiyabhama, B., Devendiran, S., Manivannan, K.: Diagnostics of Gear Faults Using Ensemble Empirical Mode Decomposition, Hybrid Binary Bat Algorithm and Machine Learning Algorithms. Journal of VibroEngineering, Volume 17, Issue 3 (2015)

[14] Jinxiu, Q., Zhousuo, Z., Teng, G.: A Novel Intelligent Method for Mechanical Fault Diagnosis Based on Dual-Tree Complex Wavelet Packet Transform and Multiple Classifier Fusion. Journal Neurocomputing, Volume 171, Issue C (2016)

[15] Večeř, P., Kreidl, M., Šmíd, R.: Condition Indicators for Gearbox Condition Monitoring Systems. ACTA POLYTECHNICA, Journal of Advanced Engineering, Volume 45, Issue 6 (2005)

[16] Večeř, P., Kreidl, M., Šmíd, R.: Gearbox Condition Monitoring Using Advanced Classifiers. ACTA POLYTECHNICA, Journal of Advanced Engineering, Volume 50, Issue 1 (2010)

[17] Sharma, V., Parey, A.: A Review of Gear Fault Diagnosis Using Various Condition Indicators, Procedia Engineering, Volume 144 (2016)

[18] Dwyer, R.: Detection of Non-Gaussian Signals by Frequency Domain Kurtosis Estimation. Proceedings of International Conference on Acoustics, Speech and Signal Processing, ICASSP-83, Volume 8 (1983)

[19] Antoni, J.: The Spectral Kurtosis: A Useful Tool for Characterizing Non-Stationary Signals. Mechanical Systems and Signal Processing, Volume. 20, Issue (2006)

[20] Bechhoefer, E., He, D., Dempsey, P.: Gear Health Threshold Setting Based on a Probability of False Alarm. Annual Conference of the Prognostics and Health Management Society (2011)

[21] Wenxian, Y., Peter J. T., Christopher, J. C., Feng, Y., Qiu, Y.: Wind Turbine Condition Monitoring: Technical and Commercial Challenges. Wind Energy, Volume 17, Issue 5 (2014)

[22] Bangalore, P., Letzgus, S., Karlsson, D., Patriksson, M.: An Artificial Neural Network-Based Condition Monitoring Method for Wind Turbines, with Application to the Monitoring of the Gearbox. Wind Energy, Volume 20, Issue 8 (2017)

[23] Bryant, L., John, A.: Modelling Wind Turbine Degradation and Maintenance. Wind Energy, Volume 19, Issue 4 (2016)
[24] David, S., Wenyu, Z., Edzel, L., AbuAli, M., Jay, L.: A Comparative Study on Vibration-Based Condition Monitoring Algorithms for Wind Turbine Drive Trains. Wind Energy, Volume 17, Issue 5 (2014)
[25] Yanhui, F., Yingning, Q., Christopher, J., Crabtree, H., L., Peter, J., T.: Monitoring Wind Turbine Gearboxes. Wind Energy, Volume 16, Issue 5 (2013)
[26] Huageng, L., Charles, H., Matthew, K., Jesse, H., Adam, W., Shuangwen, S.: Effective and Accurate Approaches for Wind Turbine Gearbox Condition Monitoring. Wind Energy, Volume 17, Issue 5(2014)
[27] Bechhoefer, E., Van Hecke, B., He, D.: Processing for Improved Spectral Analysis. Annual Conference of Prognostics and Health Management Society (2013)
[28] Mobius Institute http://www.mobiusinstitute.com, Accessed Date (2017)
[29] Nakhaeinejad, M., Bukowitz, D., O.: Practical Vibration Analysis of Machinery: Case Studies. CreateSpace Independent Publishing Platform, 2011 Edition (2011)
[30] Elforjani, M.: Estimation of Remaining Useful Life of Slow Speed Bearings Using Acoustic Emission Signals. Journal of Nondestructive Evaluation, Available Online (2016)
[31] Grigg, O., A., Farewell, V., T., Spiegelhalter, D., J.: The Use of Risk-Adjusted CUSUM and RSPRT Charts for Monitoring in Medical Contexts. Statistical Methods in Medical Research, Volume 12, Issue 2 (2003)
[32] Elforjani, M.: Diagnosis and Prognosis of Slow Speed Bearing Behaviour under Grease Starvation Condition. Structural Health Monitoring, First published date: April-28-2017.
[33] Elforjani, M., Mba, D.: Accelerated Natural Fault Diagnosis in Slow Speed Bearings with Acoustic Emission. Engineering Fracture Mechanics, Volume 77, Issue 1 (2010)